

Differential Releases of Dopamine and Neuropeptide Y from Histamine-Stimulated PC12 Cells Detected by an Aptamer-Modified Nanowire Transistor

Subhasree Banerjee, Ying-Jhu Hsieh, Chia-Rung Liu, Nai-Hsing Yeh, Hui-Hsing Hung, Yew-Seng Lai, Ai-Chuan Chou, Yit-Tsong Chen,* and Chien-Yuan Pan*

Dopamine (DA) and neuropeptide Y (NPY) are important neurotransmitters stored mainly in synaptic vesicles (SV) and large dense core vesicles (LDCV), respectively. SV and LDCV may respond differentially to various stimulations, resulting in the release of the neurotransmitters in different ratios to modulate physiological activities. However, it is difficult to monitor these neurotransmitters in real-time, especially NPY, which is usually detected by time-consuming techniques, such as the Western blot. In this study, we detected the histamine-induced NPY and DA released from pheochromocytoma 12 (PC12) cells using silicon nanowire field-effect transistors (SiNW-FETs) modified with specific aptamers against NPY and DA, respectively (referred to as APT^{NPY}/SiNW-FET and APT^{DA}/SiNW-FET).

The release of neurotransmitters from presynaptic terminals to activate the receptors at the postsynaptic neurons is the major communication pathway in the nervous system. There are three classes of neurotransmitters: amines and amino acids, both of which are usually packed into SV (≈ 50 nm in diameter),^[1] and peptides, which are stored in LDCV (100–200 nm in diameter).^[2] The elevation of the intracellular Ca²⁺ concentration triggers these two types of vesicles to fuse with the plasma membrane to release their contents into the synaptic cleft.

NPY, a 36-residue peptide stored in the LDCV, is widely distributed in the central and peripheral nervous systems.

By binding to the G-protein coupled receptors, NPY modulates various physiological activities, such as neuron survival, pain conception, learning, and memory.^[3] In addition, NPY enhances the immune response, and its presence in the serum could be a marker for cancer.^[4] DA is a catecholamine involved in various physiological activities, such as cardiovascular activity, motor control, and reward behavior.^[5] The maturation of vesicles from a cytosolic free form to a membrane-anchored release-ready form involves several steps, including translocation, docking, and priming; subsequently, Ca²⁺ triggers the last fusion process.^[6] LDCV and SV could change their respective release kinetics to modulate the synaptic plasticity.^[7] The single-cell amperometric technique could monitor DA release in real-time,^[8] but most methods, despite their good sensitivity, need to collect samples for a long duration.

PC12, a pheochromocytoma cell line derived from the adrenal medulla of rats, could differentiate to have a neuron-like morphology when induced by a nerve growth factor.^[9] In addition to DA, PC12 synthesizes and secretes several neuropeptides, such as NPY and chromogranin. It is recognized that PC12 cells store DA and NPY in a dense-cored vesicle (75–120 nm in radius), which is smaller than the LDCV in chromaffin cells (170 nm in radius).^[10] The carbon fiber amperometry technique could detect the DA secretion with a high temporal resolution at the millisecond level to resolve the fusion kinetics;^[8] in contrast, it lacks a technology to monitor the NPY secretion at the sub-second level. To date, it is still difficult to compare the releasing kinetics of NPY and DA to verify whether both NPY and DA are released under the same kinetics or not.

SiNW-FETs have emerged as a label-free, sensitive, and selective tool in the last decade.^[11] The large surface-to-volume ratio of SiNWs makes the current through the 1D nanowire highly sensitive to any electrochemical perturbation in its immediate vicinity. By means of surface functionalization with suitable receptors, SiNW-FET could detect various biomolecules with high specificity and sensitivity.^[11e,f,12] Earlier, we demonstrated the real-time detection of DA secreted from PC12 cells with a SiNW-FET modified with DA-specific aptamers.^[13] Each SiNW-FET device contains six pairs of source-drain electrodes (Sections S2 and S3 and Figures S1 and S2, Supporting Information). To modify the SiNW-FET

Dr. S. Banerjee, Y.-J. Hsieh, C.-R. Liu, Y.-S. Lai,
Prof. Y.-T. Chen
Department of Chemistry
National Taiwan University
No. 1, Sec. 4, Roosevelt Road, Taipei 106, Taiwan
E-mail: ytcchem@ntu.edu.tw

Dr. S. Banerjee, Prof. Y.-T. Chen
Institute of Atomic and Molecular Sciences
Academia Sinica
P.O. Box 23-166, Taipei 106, Taiwan

Dr. S. Banerjee, N.-H. Yeh, Dr. H.-H. Hung, Dr. A.-C. Chou, Prof. C.-Y. Pan
Department of Life Science
National Taiwan University
No. 1, Sec. 4, Roosevelt Road, Taipei 106, Taiwan
E-mail: cypan@ntu.edu.tw

DOI: 10.1002/sml.201601370



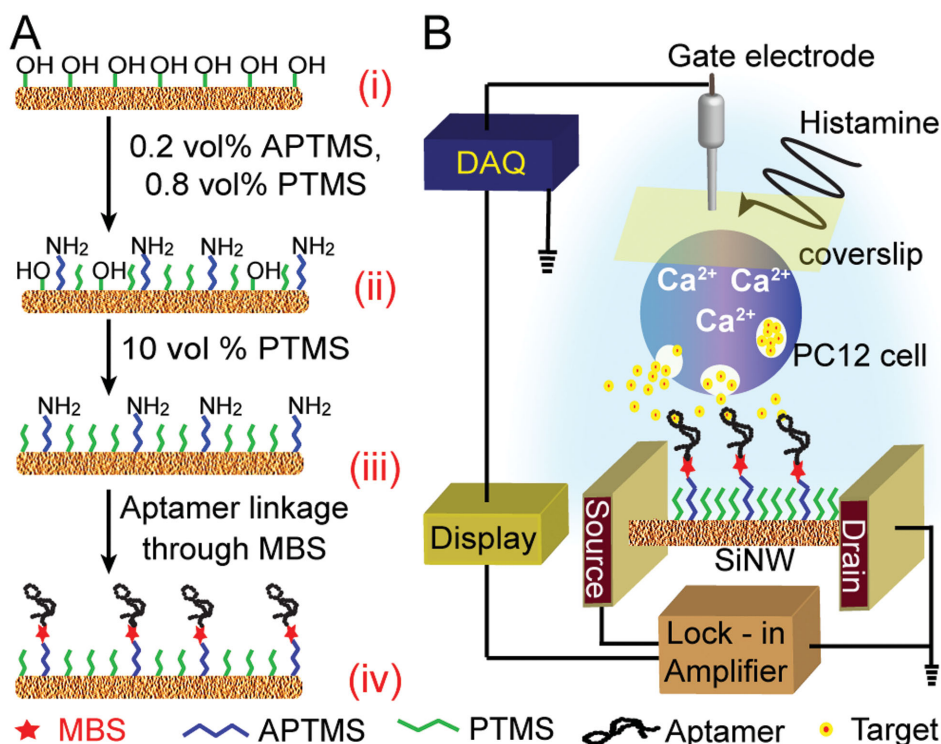


Figure 1. Schematic illustration of the experimental design. A) Surface modification of SiNW-FET with aptamers. i) Bare SiNW with free $-OH$ groups on its silica sheath. ii) Modification of the $-OH$ to $-NH_2$ groups by a mixture of APTMS:PTMS (1:4). iii) Additional PTMS modification to remove the unreacted $-OH$ groups. iv) Immobilization of aptamers to the exposed $-NH_2$ groups via an MBS linker. B) Detection of neurotransmitter release from histamine-stimulated PC12 cells.

surface with aptamers (**Figure 1**; Sections S4 and S5, Supporting Information), we first anchored 3-aminopropyltrimethoxysilane (APTMS) onto the SiNW surface, followed by linking the $-NH_2$ of APTMS to 3-maleimidobenzoic acid N-hydroxy succinimide ester (MBS). The $-NH_2$ at the 5'-terminal of the aptamer could replace the succinimide ester group of MBS. To avoid steric hindrance among the immobilized aptamers on the SiNW surface, we limited the available $-NH_2$ groups of APTMS on the SiNW by mixing the APTMS with propyltrimethoxysilane (PTMS), which is inactive to MBS.

Antibodies have a high target specificity, but their production from animals and their chemical stability in physiological buffers are inferior to those of the synthesized aptamers.^[14] Using aptamers as a receptor in FET experiments,^[15] the length of the linear aptamer conformation might exceed the effective field-effect distance (i.e., the Debye-Hückel screening length), which is ≈ 2.4 nm in $0.1 \times$ PBS buffer (phosphate-buffered saline, consisting of 13.7×10^{-3} M NaCl, 270×10^{-6} M KCl, 1×10^{-3} M Na_2HPO_4 , and 200×10^{-6} M KH_2PO_4 in NaOH, pH 7.2).^[13] The aptamer against DA contains 57 nucleotides,^[16] which is ≈ 18 nm in its linear form, and upon modification (**Figure 1A** (iv)), has a total distance of ≈ 19 nm to the SiNW-FET surface, also including the chemical linkers of MBS and APTMS. Nevertheless, because of the highly compact tertiary structure of the aptamer-DA binding site to the SiNW-FET surface becomes very short to provide a sufficient field effect to modulate the conductivity of the SiNW-FET. Similarly, the aptamer against NPY, which

contains 80 nucleotides (≈ 26 nm long), should also be packed tightly when binding NPY to ensure an effective field-effect detection.^[14]

To determine the binding affinities, we applied various concentrations of NPY and DA (denoted by C_{NPY} and C_{DA}) to the APT^{NPY}/SiNW-FET and APT^{DA}/SiNW-FET, respectively, through a microfluidic channel (**Figure 2**; Section S6, Supporting Information). As C_{NPY} (from 10×10^{-9} M to 2.5×10^{-6} M) and C_{DA} (from 100×10^{-12} M to 25×10^{-9} M) increased, the $I_{sd}-V_g$ curves shifted accordingly. The normalized ΔV_g^{cal} calculated from the $I_{sd}-V_g$ curves increased as C_{NPY} and C_{DA} increased and reached a plateau at high concentrations (**Figure 2B,D** and the corresponding semi-log plot in **Figure S3**, Supporting Information). To calculate the dissociation constant (K_d), we applied a least-squares fit of the $C/\Delta V_g^{cal}$ versus C data to the Langmuir adsorption isotherm model (Section S7, Supporting Information). The K_d for the NPY-APT^{NPY} was determined to be $295 \pm 28 \times 10^{-9}$ M, similar to the reported $\approx 300 \times 10^{-9}$ M.^[17] The $K_d = 2.43 \pm 0.23 \times 10^{-9}$ M for the DA-APT^{DA} complex is one order higher than what we reported before ($120 \pm 10 \times 10^{-12}$ M).^[13] The decrease in the binding affinity might be due to the sucrose (250×10^{-3} M) included in the $0.1 \times$ PBS buffer of this study to maintain the physiological osmolarity in the live-cell experiments (but not in the previous experiment^[13]). Sucrose molecules with their multiple $-OH$ groups might interact with NPY or DA molecules via H-bonds, which could hinder the aptamer-neurotransmitter binding. Although the K_d values of the aptamers used in this study are comparable to that of an

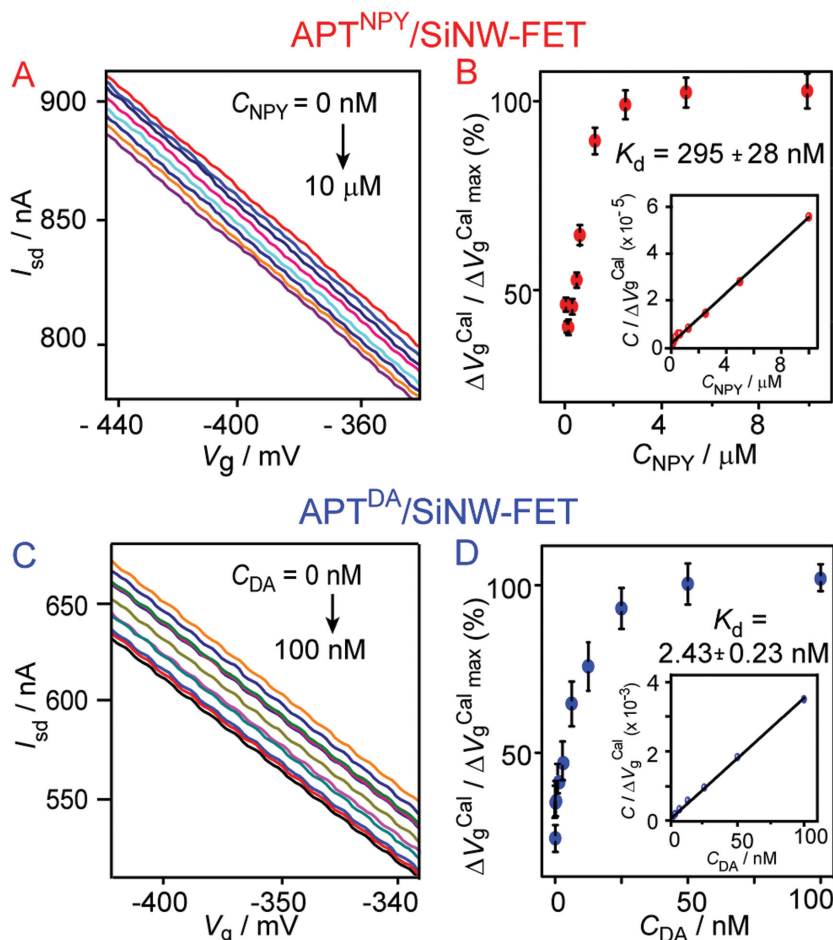


Figure 2. A,B) APT^{NPY}/SiNW-FET and C,D) APT^{DA}/SiNW-FET were perfused with various C_{NPY} and C_{DA} , respectively, to show their high binding affinities. The (A) and (C) $I_{\text{sd}}-V_{\text{g}}$ shifts, and (B) and (D) $\Delta V_{\text{g}}^{\text{cal}}/\Delta V_{\text{g,max}}^{\text{cal}}$ (%) were recorded at various C_{NPY} and C_{DA} . Insets of (B) and (C): A least-squares fit to the Langmuir adsorption isotherm model to determine the K_{d} of the aptamer-target complex. Data presented are the mean \pm standard deviation from at least three different devices.

antibody which is usually at the nm range, the binding affinity of an aptamer to target molecules could be enhanced by a refinement selection protocol. In addition, a multivalent aptamer could be constructed to recognize multiple epitopes of a target molecule to improve not only the binding affinity but also target selectivity.^[18] By varying the nucleotide sequence, an aptamer can be easily adjusted its binding property, which provides an advantage over traditional antibody receptors produced from animals. Therefore, aptamers are suitable receptor molecules to be used in a SiNW-FET biosensor for detecting specific biomarkers.

Histamine is not only a neurotransmitter in the nervous system but also a signaling molecule involved in various physiological functions.^[19] By binding to the corresponding G protein-coupled receptors, histamine activates several signaling pathways, including the IP₃ receptor at the endoplasmic reticulum to release Ca²⁺ into the cytosol, resulting in the fusion of the SV and LDCV with the plasma membrane.^[20] To monitor the secretion of NPY and DA from the PC12 cells (Section S8, Supporting Information), we placed the cells atop the APT^{NPY}/SiNW-FET and APT^{DA}/SiNW-FET,

respectively, and sequentially added various concentrations of histamine (C_{Hist}) to the cells to induce secretion. Histamine (25×10^{-6} M) without cells had no apparent effect on the ΔG of APT^{NPY}/SiNW-FET or APT^{DA}/SiNW-FET (Figure S4, Supporting Information). In the presence of cells, the ΔG s of both APT^{NPY}/SiNW-FET and APT^{DA}/SiNW-FET decreased upon the addition of histamine (Figure 3A,D). The normalized ΔG of the APT^{NPY}/SiNW-FET showed a significant response at $C_{\text{Hist}} \approx 1 \times 10^{-6}$ M and reached a saturation level at $\approx 3 \times 10^{-6}$ M (Figure 3C). In contrast, the normalized ΔG of APT^{DA}/SiNW-FET did not show any apparent change until $C_{\text{Hist}} > 2 \times 10^{-6}$ M and reached a plateau at $>10 \times 10^{-6}$ M (Figure 3F). The $I_{\text{sd}}-V_{\text{g}}$ curves shifted downward as the C_{Hist} increased for both APT^{NPY}/SiNW-FET and APT^{DA}/SiNW-FET (Figure 3B,E). By plotting the $\Delta V_{\text{g}}^{\text{cal}}/\Delta V_{\text{g,max}}^{\text{cal}}$ (%) against C_{Hist} (Figure 3C,F), the EC₅₀ of histamine in releasing NPY and DA was determined to be 1.6 ± 0.2 and $4.6 \pm 0.4 \times 10^{-6}$ M, respectively.

Compared with the DA release at higher C_{Hist} (Figure 3F), one possibility why the ΔG of APT^{NPY}/SiNW-FET reaches a plateau at a lower C_{Hist} (Figure 3C) is that the large-quantity release of NPY saturates all the binding sites. However, by comparing the curves of $\Delta V_{\text{g}}^{\text{cal}}$ versus C_{Hist} in Figure 3C and $\Delta V_{\text{g}}^{\text{cal}}$ versus C_{NPY} in Figure 2C (summarized in Figure S5, Supporting Information with the measured $\Delta V_{\text{g}}^{\text{cal}}$ in the same units (mV) for easier comparison), the response of the APT^{NPY}/

SiNW-FET to the histamine-induced NPY release from cells (Figure 3C) is well below that induced by direct NPY application (Figure 2C). Therefore, it is unlikely that the NPY released from the cells saturated the binding sites on the APT^{NPY}/SiNW-FET. The APT^{NPY} also has a much lower affinity in binding NPY ($K_{\text{d}} = 295 \pm 28 \times 10^{-9}$ M) than the APT^{DA} does to DA ($K_{\text{d}} = 2.43 \pm 0.23 \times 10^{-9}$ M). Consequently, the NPY detected at low C_{Hist} stimulation is not due to the saturation of the APT^{NPY}/SiNW-FET but suggests that the LDCV and SV respond differentially to C_{Hist} at different levels (Figure 3C,F).

Under physiological condition as C_{Hist} rises from a basal level, the neuroendocrine cell would release NPY first, and then the DA. Different types of histamine receptors have different affinities to histamine; both the H₁ and H₂ receptors are in the μM range, whereas the H₃ and H₄ receptors are in the low nm range.^[21] While the H₁ and H₄ receptors are capable of releasing Ca²⁺ from their intracellular stores, others can modulate neuron activities. These receptors work cooperatively in different combinations to determine what vesicles are to be released at various C_{Hist} . Henceforth, low and high C_{Hist} can stimulate the releases of signaling

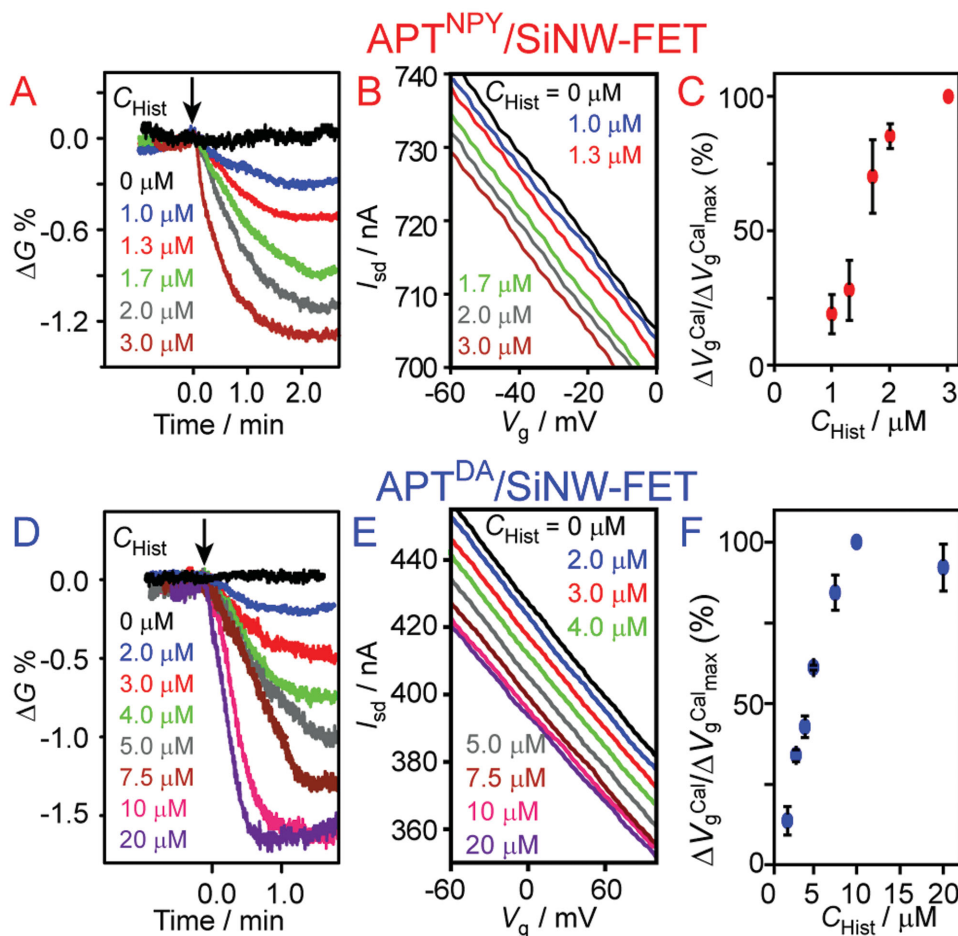


Figure 3. A–C) APT^{NPY}/SiNW-FET and D–F) APT^{DA}/SiNW-FET were used to detect the histamine-evoked NPY and DA secretions from PC12 cells with various C_{Hist} . Measured (A) and (D) real-time ΔG , (B) and (E) $I_{\text{sd}}-V_g$ shifts, and (E) and (F) $\Delta V_{\text{g,Cal}}/\Delta V_{\text{g,Cal,max}}$ (%) changes as a function of C_{Hist} . Data presented are the mean \pm standard deviation from at least three different devices.

molecules from various types of vesicles in different combinations to modulate physiological functions.

PC12 cells express several types of DA receptor, whose activation could result in the inhibition of NPY release.^[22] To verify the APT^{NPY}/SiNW-FET capable of discriminating the DA-induced inhibition of NPY release, we repetitively stimulated the PC12 cells with histamine (1.7×10^{-6} M) three times but without treating with DA (Figure 4A; Figure S6A, Supporting Information); comparatively, we treated the cells with DA (20×10^{-6} M) during the 2nd stimulation (Figure 4B; Figure S6B, Supporting Information). After each stimulation, we incubated the cells in HBSS for 5 min and washed away the DA. Figure 4A shows that the histamine induced a similar level of ΔG during the three consecutive stimulations. However, for the cells treated with DA during the 2nd stimulation (Figure 4B), the ΔG was greatly suppressed in the subsequent 2nd and 3rd stimulations, even though the DA had been washed off

before the 3rd stimulation. As summarized in Figure 4C and Figure S6 (Supporting Information), the average ΔG s of the

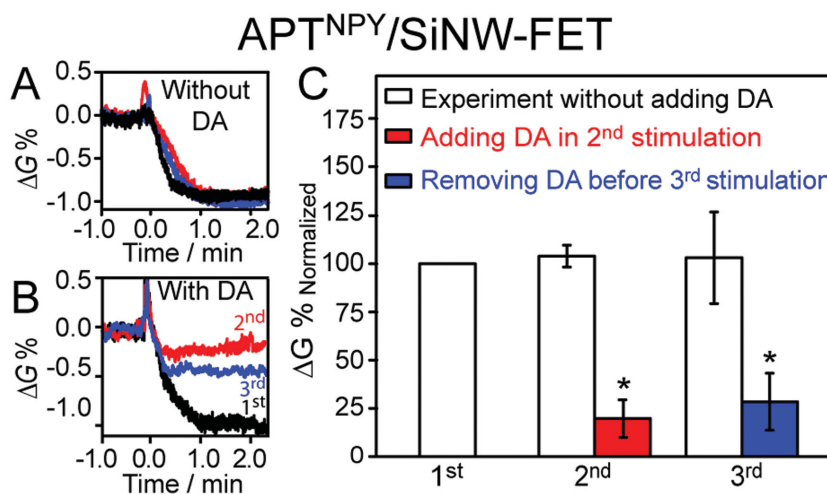


Figure 4. Real-time ΔG s measured for three consecutive histamine (1.7×10^{-6} M) stimulations A) without DA and B) with DA (20×10^{-6} M) treatment during the 2nd stimulation. C) Normalized ΔG for the three stimulations. Data presented are the mean \pm standard deviation from four different devices; the statistical significance was analyzed by the Mann–Whitney U test; *, $p < 0.05$.

2nd and 3rd stimulations, relative to the control experiment of the 1st stimulation without DA treatment, are $104 \pm 5.71\%$ and $103 \pm 23.8\%$ ($n = 4$), respectively. After the DA treatment, the 2nd and 3rd histamine-evoked ΔG_s were significantly suppressed to $19.8 \pm 9.60\%$ ($n = 4$, $p < 0.05$) and $28.4 \pm 14.8\%$ ($n = 4$, $p < 0.05$), respectively. As a result, our FET device is sensitive to discriminate the modulatory effect of signaling molecules in the NPY release.

The sensitivity of the APT^{NPY}/SiNW-FET toward NPY is reduced almost by half when the sample contained 20×10^{-6} M of DA (Figure S7, Supporting Information). Since the same device did not suffer from the interference of DA at 100×10^{-9} M (Figure S8, Supporting Information), the reduced sensitivity was probably due to nonspecific binding, or the interference from abundant DA which hinders the NPY-APT^{NPY} interaction. However, the inhibitory effect of DA on the NPY release (Figure 4C; Figure S6B, Supporting Information) was more than 50%. Moreover, the inhibitory effect on the NPY release still remained in the 3rd stimulation, even though the DA was washed away. DA modulates various signaling pathways, such as the Ca²⁺-dependent protein kinase activity, through G-protein coupled receptors, and this effect could last for a long period of time. Histamine (1.7×10^{-6} M) induces an apparent NPY release, but little DA secretion (Figure 3C,F); henceforth, the DA secreted by PC12 cells at high C_{Hist} would raise the local C_{DA} surrounding the cells and become a feedback factor to attenuate the NPY release. The saturation level of NPY released from the PC12 cells at $C_{\text{Hist}} > 3 \times 10^{-6}$ M may be partially due to the inhibitory effect of the DA released. Consequently, our device is capable of studying the physiological modulation of exocytotic events.

Every neuron releases multiple neurotransmitters simultaneously to modulate the synaptic plasticity; however, it is difficult to monitor these molecules on the same time scale.^[23] The existing carbon fiber amperometric technique could resolve the DA secretion at the level of single exocytotic events;^[8] however, it takes time to collect enough samples for a Western blot or mass spectrometry to analyze the neuropeptide released. Here, we report the first immediate detection of NPY secreted from living PC12 cells using APT^{NPY}/SiNW-FET. In addition, we verify that the C_{Hist} to excite the NPY release from PC12 cells is lower than that required to stimulate the DA release. Therefore, it is possible that NPY and DA are stored in different types of vesicles. Such differential concentration dependence is an important modulation mechanism to control the signaling pathways for various physiological activities. In addition to the sensitivity and specificity of the SiNW-FET biosensor in detecting target molecules, this device can further be applied to monitoring the kinetics of the release of neurotransmitters to understand how neurons co-release these signaling molecules to modulate the synaptic plasticity.

Supporting Information

Supporting Information is available from the Wiley Online Library or from the author.

Acknowledgements

This work was supported by the Ministry of Science and Technology of Taiwan under Grant Nos. 104-2627-M-002-002 (Y.-T.C.) and 104-2627-M-002-003 (C.-Y.P.) & 103-2320-B-002-060-MY3 (C.-Y.P.). Technical support from NanoCore, the Core Facilities for Nanoscience and Nanotechnology at Academia Sinica, is also acknowledged.

- [1] M. C. Gondré-Lewis, J. J. Park, Y. P. Loh, *Int. Rev. Cell. Mol. Biol.* **2012**, *299*, 27.
- [2] a) W. P. de Potter, L. Dillen, W. Annaert, K. Tombeur, R. Berghmans, E. P. Coen, *Synapse* **1988**, *2*, 157; b) J. B. Papke, J. M. Moore-Dotson, D. J. Watson, C. D. Wedell, L. R. French, S. R. Rendell, A. B. Harkins, *Neuroscience* **2012**, *218*, 78.
- [3] a) Y. Dumont, J.-C. Martel, A. Fournier, S. St-Pierre, R. Quirion, *Prog. Neurobiol.* **1992**, *38*, 125; b) É. Borbély, B. Scheich, Z. Helyes, *Neuropeptides* **2013**, *47*, 439.
- [4] a) M. Czarnecka, E. Trinh, C. Lu, A. Kuan-Celarier, S. Galli, S.-H. Hong, J. U. Tilan, N. Talisman, E. Izycka-Swieszewska, J. Tsuei, C. Yang, S. Martin, M. Horton, D. Christian, L. Everhart, I. Maheswaran, J. Kitlinska, *Oncogene* **2015**, *34*, 3131; b) K. Ueda, A. Tatsuguchi, N. Saichi, A. Toyama, K. Tamura, M. Furihata, R. Takata, S. Akamatsu, M. Igarashi, M. Nakayama, T.-A. Sato, O. Ogawa, T. Fujioka, T. Shuin, Y. Nakamura, H. Nakagawa, *J. Proteome Res.* **2013**, *12*, 4497.
- [5] a) J. D. Salamone, M. Correa, *Neuron* **2012**, *76*, 470; b) V. S. Chakravarthy, D. Joseph, R. S. Bapi, *Biol. Cybern.* **2010**, *103*, 237; c) R. A. Wise, *Nat. Rev. Neurosci.* **2004**, *5*, 483.
- [6] V. Haucke, E. Neher, S. J. Sigrist, *Nat. Rev. Neurosci.* **2011**, *12*, 127.
- [7] Y. Park, K.-T. Kim, *Cell. Signal.* **2009**, *21*, 1465.
- [8] S. E. Zerby, A. G. Ewing, *Brain Res.* **1996**, *712*, 1.
- [9] R. H. S. Westerink, A. G. Ewing, *Acta Physiol.* **2008**, *192*, 273.
- [10] Z. Zhang, Y. Wu, Z. Wang, F. M. Dunning, J. Rehffuss, D. Ramanan, E. R. Chapman, M. B. Jackson, *Mol. Bio. Cell* **2011**, *22*, 2324.
- [11] a) Y. Cui, Q. Wei, H. Park, C. M. Lieber, *Science* **2001**, *293*, 1289; b) J.-I. Hahm, C. M. Lieber, *Nano Lett.* **2004**, *4*, 51; c) F. Patolsky, B. P. Timko, G. Yu, Y. Fang, A. B. Greytak, G. Zheng, C. M. Lieber, *Science* **2006**, *313*, 1100; d) F. Patolsky, G. Zheng, O. Hayden, M. Lakadamyali, X. Zhuang, C. M. Lieber, *Proc. Natl. Acad. Sci. USA* **2004**, *101*, 14017; e) T.-W. Lin, P.-J. Hsieh, C.-L. Lin, Y.-Y. Fang, J.-X. Yang, C.-C. Tsai, P.-L. Chiang, C.-Y. Pan, Y.-T. Chen, *Proc. Natl. Acad. Sci. USA* **2010**, *107*, 1047; f) Y. Wang, T. Wang, P. Da, M. Xu, H. Wu, G. Zheng, *Adv. Mater.* **2013**, *25*, 5177.
- [12] a) Z. Li, Y. Chen, X. Li, T. I. Kamins, K. Nauka, R. S. Williams, *Nano Lett.* **2004**, *4*, 245; b) T.-S. Pui, A. Agarwal, F. Ye, Y. Huang, P. Chen, *Biosens. Bioelectron.* **2011**, *26*, 2746; c) G.-J. Zhang, G. Zhang, J. H. Chua, R.-E. Chee, E. H. Wong, A. Agarwal, K. D. Buddharaju, N. Singh, Z. Gao, N. Balasubramanian, *Nano Lett.* **2008**, *8*, 1066; d) G. Zheng, X. P. A. Gao, C. M. Lieber, *Nano Lett.* **2010**, *10*, 3179; e) A. Gao, N. Lu, Y. Wang, P. Dai, T. Li, X. Gao, Y. Wang, C. Fan, *Nano Lett.* **2012**, *12*, 5262; f) N. Lu, A. Gao, P. Dai, S. Song, C. Fan, Y. Wang, T. Li, *Small* **2014**, *10*, 2022; g) G.-J. Zhang, M. J. Huang, J. J. Ang, Q. Yao, Y. Ning, *Anal. Chem.* **2013**, *85*, 4392.
- [13] B.-R. Li, Y.-J. Hsieh, Y.-X. Chen, Y.-T. Chung, C.-Y. Pan, Y.-T. Chen, *J. Am. Chem. Soc.* **2013**, *135*, 16034.
- [14] F. Tolle, G. Mayer, *Chem. Sci.* **2013**, *4*, 60.
- [15] J. Kim, Y. S. Rim, H. Chen, H. H. Cao, N. Nakatsuka, H. L. Hinton, C. Zhao, A. M. Andrews, Y. Yang, P. S. Weiss, *ACS Nano* **2015**, *9*, 4572.

- [16] a) C. Mannironi, A. D. Nardo, P. Fruscoloni, G. P. Tocchini-Valentini, *Biochemistry* **1997**, *36*, 9726; b) R. Walsh, M. C. DeRosa, *Biochem. Biophys. Res. Commun.* **2009**, *388*, 732.
- [17] S. D. Mendonsa, M. T. Bowser, *J. Am. Chem. Soc.* **2005**, *127*, 9382.
- [18] H. Hasegawa, N. Savory, K. Abe, K. Ikebukuro, *Molecules* **2016**, *21*, 421.
- [19] H. L. Haas, O. A. Sergeeva, O. Selbach, *Physiol. Rev.* **2008**, *88*, 1183.
- [20] N. Gustavsson, W. Han, *Biosci. Rep.* **2009**, *29*, 245.
- [21] R. L. Thurmond, E. W. Gelfand, P. J. Dunford, *Nat. Rev. Drug Discov.* **2008**, *7*, 41.
- [22] a) G. Cao, A. Gardner, T. C. Westfall, *Biochem. Pharmacol.* **2007**, *73*, 1446; b) X. Chen, T. C. Westfall, *Am. J. Physiol. Cell Physiol.* **1994**, *266*, C784.
- [23] T. S. Hnasko, R. H. Edwards, *Annu. Rev. Physiol.* **2012**, *74*, 225.

Received: April 21, 2016
Revised: July 21, 2016
Published online: August 23, 2016



Supporting Information

for *Small*, DOI: 10.1002/sml.201601370

Differential Releases of Dopamine and Neuropeptide Y from Histamine-Stimulated PC12 Cells Detected by an Aptamer-Modified Nanowire Transistor

Subhasree Banerjee, Ying-Jhu Hsieh, Chia-Rung Liu, Nai-Hsing Yeh, Hui-Hsing Hung, Yew-Seng Lai, Ai-Chuan Chou, Yit-Tsong Chen, and Chien-Yuan Pan**

Supporting Information

Differential Releases of Dopamine and Neuropeptide Y from Histamine-Stimulated PC12 Cells Detected by an Aptamer-Modified Nanowire Transistor

Subhasree Banerjee, Ying-Jhu Hsieh, Chia-Rung Liu, Nai-Hsing Yeh, Hui-Hsing Hung, Yew-Seng Lai, Ai-Chuan Chou, Yit-Tsong Chen, Chien-Yuan Pan**

Dr. S. Banerjee, Y.-J. Hsieh, C.-R. Liu, Y.-S. Lai, Prof. Y.-T. Chen
Department of Chemistry, National Taiwan University, No. 1, Sec. 4, Roosevelt Road, Taipei 106, Taiwan
E-mail: ytchem@ntu.edu.tw

Dr. S. Banerjee, Prof. Y.-T. Chen
Institute of Atomic and Molecular Sciences, Academia Sinica, P.O. Box 23-166, Taipei 106, Taiwan

Dr. S. Banerjee, Dr. N.-H. Yeh, Dr. H.-H. Hung, Dr. A.-C. Chou, Prof. C.-Y. Pan
Department of Life Science, National Taiwan University, No. 1, Sec. 4, Roosevelt Road, Taipei 106, Taiwan
E-mail: cypan@ntu.edu.tw

Keywords: dopamine, neuropeptide Y, histamine, large dense-core vesicle, silicon nanowire field-effect transistor

S1. Materials

Reagents for cell culture were purchased from InVitrogen Inc. (Carlsbed, CA, USA). All chemicals were purchased from Sigma-Aldrich Inc. (St. Louis, MO, USA), unless otherwise indicated. Sodium citrate dihydrate ($\text{HOC}(\text{COONa})(\text{CH}_2\text{COONa})_2 \cdot 2\text{H}_2\text{O}$, ACS grade) was obtained from Macron Chemicals (Center Valley, USA). Hydrogentetrachloroaurate (III) trihydrate ($\text{HAuCl}_4 \cdot 3\text{H}_2\text{O}$, ACS grade), and dopamine (DA) were purchased from Acros Organics Inc. (New Jersey, USA) Neuropeptide Y (NPY) were purchased from TOCRIS (Pittsburgh, USA) and sucrose was obtained from Macron Fine Chemicals (Center Valley, USA). Dithiothreitol (DTT) was purchased from J. T. Baker (Center Valley, USA). Single-strain DNA-aptamers and a FITC-labeled aptamer (referred to as FITC-aptamer) were purchased from Protech Technology (Taipei, Taiwan); the nucleotide sequence of the aptamers specific for NPY and DA were AGC AGC ACA GAG GTC AGA TGC AAA CCA CAG CCT GAG TGG TTA GCG TAT GTC ATT TAC GGA CCT ATG CGT GCT ACC GTG AA^[S1] and 5'-GTC TCT GTG TGC GCC AGA GAC ACT GGG GCA GAT ATG GGC CAG CAC AGA ATG AGG CCC-3',^[S2] respectively. An amino group was modified at the 5' end of each oligonucleotides; the FITC was modified at the 3' end of the NPY aptamer. All chemicals were ACS reagents.

S2. Synthesis of SiNW

S2.1. Synthesis of Au nanoparticles

Highly monodispersed Au nanoparticles of ~20 nm in diameter were synthesized using the standard procedures pioneered by Frens.^[S3] In this method, we first prepared the stock solutions of HAuCl_4 (3 mM) and trisodium citrate (38.8 mM) in deionized water and then diluted the HAuCl_4 (5 mL) with deionized water (10 mL) under a stirring condition on a hot plate. When boiling, we added trisodium citrate (~0.75 mL) dropwise until the solution

changed color from blue to burgundy, indicating the formation of monodispersed Au nanoparticles.

S2.2. Synthesis of SiNWs

We applied a bottom-up technique to fabricate boron-doped p-type SiNWs (Si:B = 4000:1).^[S4-S7] Single-crystalline SiNWs were grown in a chemical vapor deposition (CVD) reaction following the vapor-liquid-solid growth mechanism, which was catalytically assisted by the as-synthesized Au nanoparticles (~20 nm in diameter). Prior to the growth of the SiNWs, a Si wafer with an oxide layer (400 nm in thickness) was cleaned in oxygen plasma (100 W, 50 sccm O₂, 200 s). The plasma-cleaned wafer was immersed in an aqueous solution containing 0.1 % poly-L-lysine for 2 min to modify its surface with a self-assembled monolayer (SAM)^[S6] of poly-L-lysine. The Si wafer was rinsed with water, dried under N₂ flow, and then transferred to the solution containing Au nanoparticles (~20 nm in diameter) for 5 s to let the poly-L-lysine SAM attract Au nanoparticles. The Au nanoparticle-deposited Si wafer was washed with deionized water, dried under N₂ flow, and then cleaned in oxygen plasma (100 W, 50 sccm O₂, 300 s). The synthetic conditions used for the CVD growth of p-type SiNWs were 455 °C for 30 min in 20 sccm Ar, 6 sccm SiH₄ (99.999 %), and 12 sccm B₂H₆ (100 ppb in H₂) at a total chamber pressure of 25 torr. The length and diameter of the SiNWs are ~20–30 μm and ~20–30 nm, respectively (Figure S1A). The as-synthesized SiNWs have a silica sheath of ~2–3 nm in thickness (Figure S1B).

S3. Device fabrication of SiNW-FETs

The SiNWs were aligned within a lithography-defined region on a photoresist (S1805)-coated Si wafer with an oxide layer (400 nm in thickness) using a contact printing method.^[S8] We placed hundreds of p-type single-crystalline SiNWs (~20 nm in diameter each) to link the comb-shaped electrodes (Figure S1C). In the device fabrication, the SiNWs-containing Si wafer was coated with photoresist layers of LOR5B and S1813, respectively. The metal

contact regions were defined on the photoresists-coated Si wafer by standard lithographic procedures and were cleaned with oxygen plasma (100 W, 50 sccm, 60 s). The silica sheath on SiNW in the contact area (with electrodes) was removed with a buffered oxide etching solution (6:1 volume ratio of 40 % NH_4F in water to 49 % HF in water). A thermal evaporation method was used to deposit metal layers of Ni (70 nm) and Al (100 nm) consecutively, as the source and drain electrodes, on the metal contact areas defined by lithography. Between the source and drain electrodes, the distance was maintained at 3 μm (Figure S1C). The SiNW-FET devices were further annealed in forming gas (10 % H_2 and 90 % N_2) at 360 °C for 3 min after the removal of photoresist to achieve a good electrical contact between SiNWs and the metal electrodes. We applied a bias voltage (V_{sd}) in a ramp pattern across the paired electrodes and obtained a linear current (I_{sd}) vs. V_{sd} curve, indicating no apparent Schottky barrier (Figure S2A). The I_{sd} vs. back gate voltage (V_{g}) indicates the sensitive, prominent p-type field effect of the device (Figure S2B).

S4. Surface modification of SiNW-FETs

The surface of SiNW-FET was cleaned with oxygen plasma (25 W, 50 sccm, 60 s) and then conjugated for 15 min with APTMS (0.2 vol %) and PTMS (0.8 vol %) at a ratio of 1:4. Subsequently, the device was rinsed with ethanol, dried under N_2 flow, and heated at 110 °C for 15 min to ensure the formation of Si-O-Si linkage between the SiNW surface and the adsorbed SAM of APTMS and PTMS. To prevent non-specific bindings at the Si-OH groups on the SiNW surface during the sensing measurements with SiNW-FETs, the device was treated with an ethanol solution containing 10 % PTMS for 15 min, rinsed with ethanol, and dried in an oven at 110 °C for 15 min. The device was then incubated in 1 mM of MBS solution (1:9 volume mixture of dimethyl sulfoxide (DMSO) and 1 \times PBS) for 30 min, rinsed with deionized water, and dried under N_2 flow. The MBS-modified device was incubated in 1 \times PBS containing 10 μM of aptamer-S-S-aptamer and 100 mM of dithiothreitol (DTT)

solution (to cleave the disulfide linkage) for 4 h. The sulfhydryl linked DNA aptamer reacted with the maleimide group of MBS to form an aptamer-modified SiNW-FET device. The aptamers-immobilized SiNW-FETs are referred to as APT^{NPY}/SiNW-FET and APT^{DA}/SiNW-FET when specific aptamers against NPY and DA were modified, respectively.

S5. Fluorescence images of an FITC-aptamer-anchored SiNW-FET device

To verify the anchorage of aptamers onto SiNWs, we used an NPY-specific aptamer labeled with an FITC at the 3' end and an amino group at the 5' end to be modified on an APTMS-immobilized SiO₂/Si substrate via a chemical linker of MBS. First, the APTMS-immobilized SiO₂/Si substrate was incubated in 1 mM MBS solution (1:9 volume mixture of DMSO and 1× PBS) for 30 min and then rinsed with deionized water and dried under N₂ flow. Subsequently, the MBS-modified SiO₂/Si substrate was incubated with the FITC-aptamers (1 μM) for 2 h. After cleaning the SiO₂/Si substrate with deionized water and drying under N₂ flow, the fluorescence emitted from the immobilized FITC-aptamers (as shown in Figure S1D) was visualized by placing the SiO₂/Si substrate on an upright fluorescence microscope (Axioplan 2, Zeiss) equipped with an intensified Cool Snap EZ charged coupled device (CCD) camera (EZ, Princeton). The homogeneous fluorescence intensity indicates the successful covalent bonding of the FITC-labeled aptamers to the SiO₂/Si surface, while the region without modification remained dark.

S6. Electrical measurement

In all sensing measurements, the source-drain current (I_{sd}) vs. gate voltage (V_g) curves and the I_{sd} vs. time (t) plots were recorded with a lock-in amplifier (SR830, Stanford Research System) operating at the source-drain voltage (V_{sd}) of 10 mV, a modulation frequency of 79 Hz, and a time constant of 100 ms. The V_g was applied in a ramp form (-0.5 to 0.5 V, 0.05 mV/s) to induce a current change in SiNW-FETs. In biosensing measurements, the samples were dissolved in 0.1× PBS (with the Debye-Hückel length of ~2.4 nm), which is long

enough to cover the distance from the binding sites to SiNW-FET surface (~2 nm) to enable the effective detection of electrical signals without severe electrolytic screening. The analytes were either delivered to the sensing SiNW-FETs through a polydimethylsiloxane (PDMS) microfluidic channel (6.26 mm (length) × 500 μm (width) × 50 μm (height)) driven by a syringe pump (KD-101, KD Scientific) (Figure S1E) or added directly to the solution in a PDMS well on a SiNW-FET device (Figure S1F). An Ag/AgCl electrode was used as a solution gate, where voltage was supplied by a data acquisition system (DAQ-NI2110, National Instruments) and was maintained at ground potential to minimize electrical noise throughout the real-time electrical measurements. The same SiNW-FET device was used to construct the calibrated response curves.

S7. Dissociation constant

The dissociation constant (K_d) of the aptamer-target complex was determined by a least-square fit of the ΔV_g^{cal} vs. C (concentration) data to the Langmuir adsorption isotherm model.^[S4, S5, S9, S10]

$$\frac{C}{\Delta V_g^{cal}} = \frac{1}{\Delta V_{g, \max}^{cal}} C + \frac{1}{\Delta V_{g, \max}^{cal}} K_d \quad (1)$$

where

$$\Delta V_g^{cal} (\%) = \frac{\Delta V_g^{cal} - \Delta V_{g,0}^{cal}}{\Delta V_{g, \max}^{cal} - \Delta V_{g,0}^{cal}} \times 100 (\%) \quad (2)$$

$\Delta V_{g,0}^{cal}$ is the calibrated response at $C = 0$ M, at which no signal was detected. $\Delta V_{g, \max}^{cal}$ is the calibrated responses in the presence of target molecules at a concentration with maximal response.

S8. Culture and stimulation of PC12 cells

The PC12 cells were cultured in Dulbecco's modified Eagle's medium containing 10 % horse serum and 5 % fetal bovine serum, and incubated at 37 °C in a humidified atmosphere with 10 % CO₂. The medium was changed on alternate days. The cultured cells were re-

suspended in medium and seeded onto the surface of a glass coverslip coated with poly-L-lysine. The glass coverslip was laid atop APT^{NPY}/SiNW-FET or APT^{DA}/SiNW-FET, with the cells facing the FET device. The cells were incubated in 0.1× PBS (13.7 mM NaCl, 270 μM KCl, 1 mM Na₂HPO₄, and 180 μM KH₂PO₄, pH 7.2) containing 250 mM sucrose; different concentrations of histamine (C_{Hist}) were added directly into the buffer to stimulate the cells. Between each stimulation, we incubated the cells in Hanks' balanced salt solution (HBSS, 1.26 mM CaCl₂, 5.33 mM KCl, 440 μM KH₂PO₄, 500 μM MgCl₂, 410 μM MgSO₄, 138 mM NaCl, 4 mM NaHCO₃, 300 μM Na₂HPO₄, and 5.6 mM glucose, pH 7.4) for 5 min.

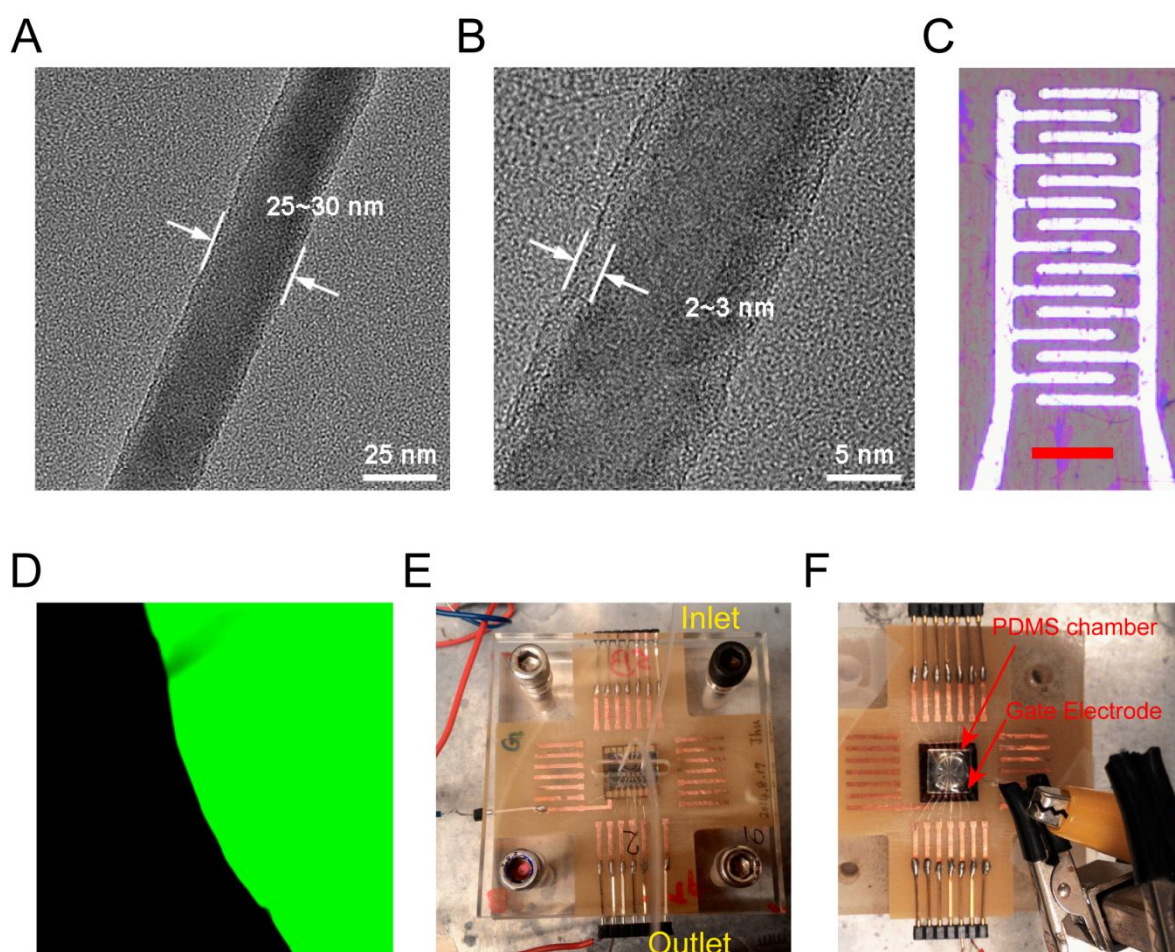


Figure S1. Images of the SiNW-FET device. A–B) HR-TEM images of p-type crystalline SiNWs (scale bar: 25 nm). The diameters of the SiNWs were generally between 20 and 30 nm. The silica sheath on a SiNW is typically of ~2–3 nm in thickness (scale bar: 5 nm). C) A pair of the comb-like source-drain electrodes (top view, scale bar: 10 nm). D) The green fluorescence indicates the successful anchorage of the FITC-labeled aptamers onto the Si wafer. E–F) During the biosensing experiments, analytes were delivered through a PDMS microfluidic channel to the SiNW-FET device or dropped into a PDMS well located at the center of the SiNW-FET device to accommodate a coverslip grown with PC12 cells.

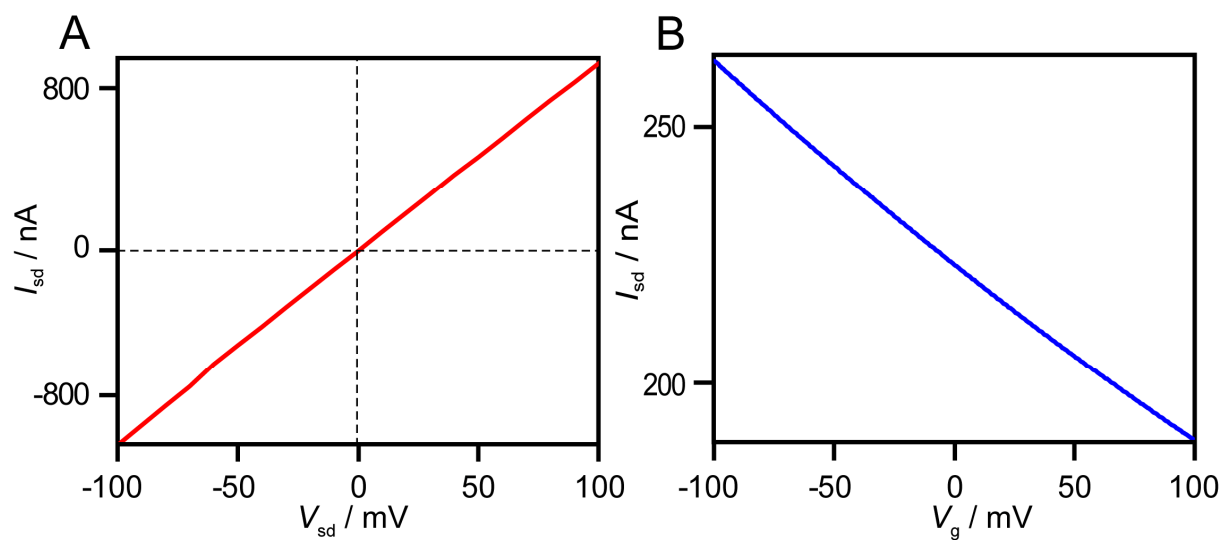


Figure S2. Electrical characterizations of a SiNW-FET device. A) Output curve (I_{sd} - V_{sd}) measured in ambient conditions with $V_g = 0$ V. B) Transfer curve (I_{sd} - V_g) measured in $0.1\times$ PBS buffer at $V_{sd} = 10$ mV.

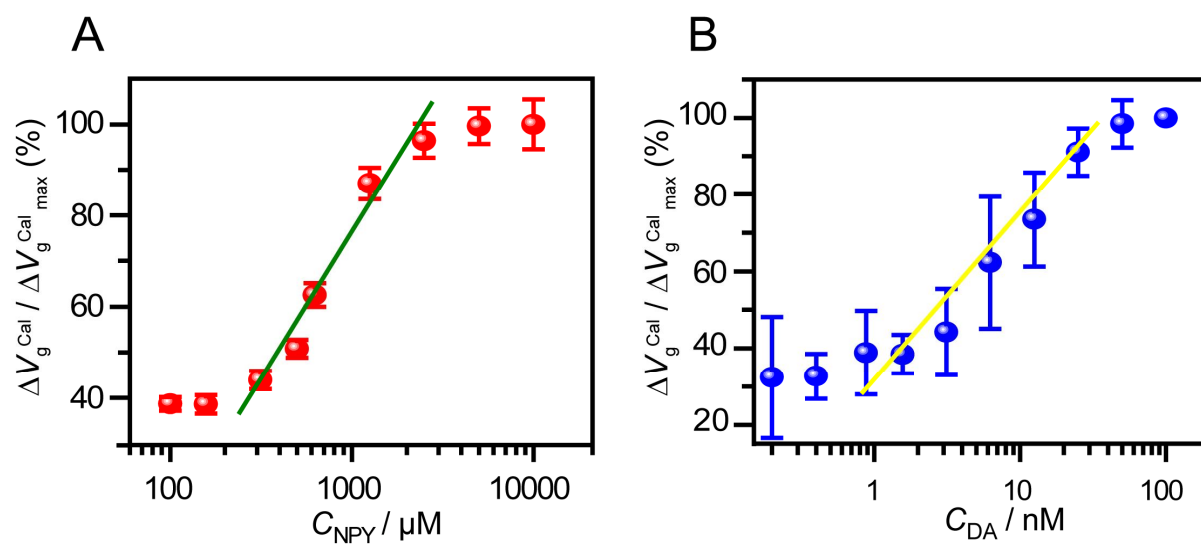


Figure S3. Semi-log plots of measured $\Delta V_g^{cal} / \Delta V_{g,max}^{cal}$ (%) as a function of A) C_{NPY} and B) C_{DA} .

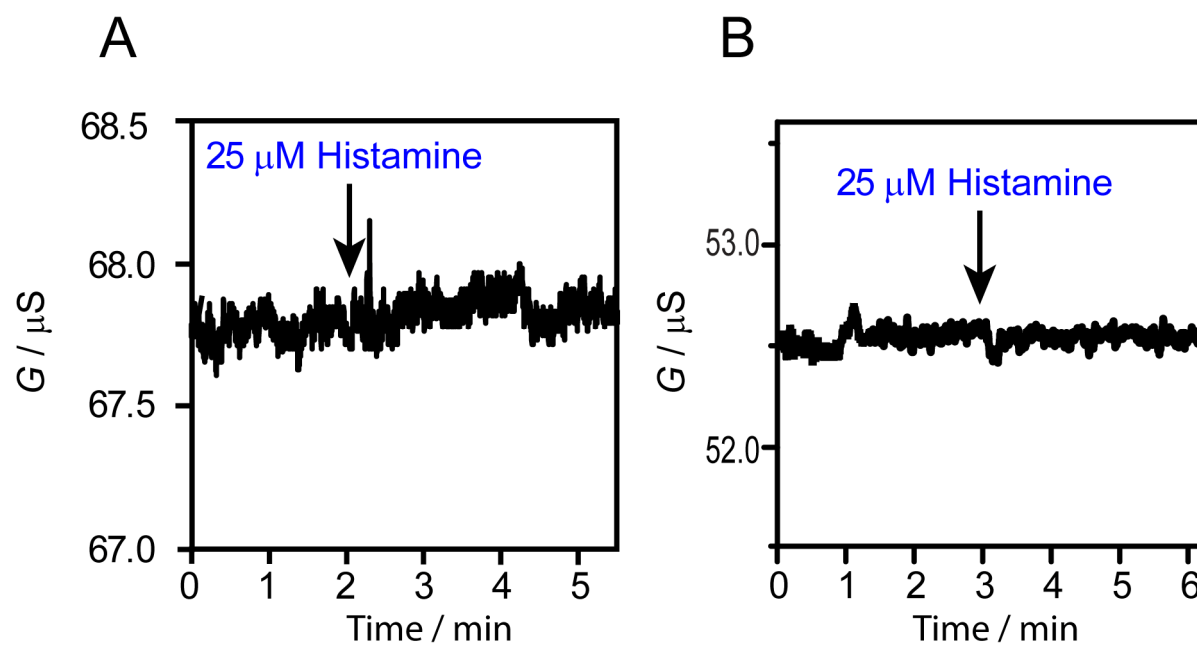


Figure S4. The addition of histamine has no effect on the electrical conductance (G) of A) an $\text{APT}^{\text{NPY}}/\text{SiNW-FET}$ and B) an $\text{APT}^{\text{DA}}/\text{SiNW-FET}$.

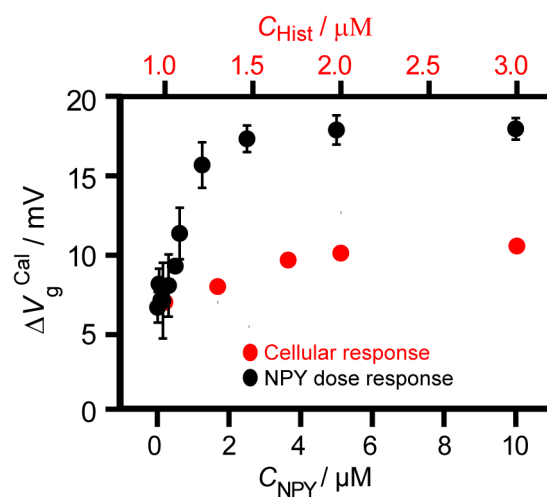


Figure S5. Comparison of the calibrated responses. The calibrated responses (ΔV_g^{cal}) of an $\text{APT}^{\text{NPY}}/\text{SiNW-FET}$ to the targeted NPY molecules of known C_{NPY} (black data points) and histamine-evoked secretion (red data points) are plotted altogether.

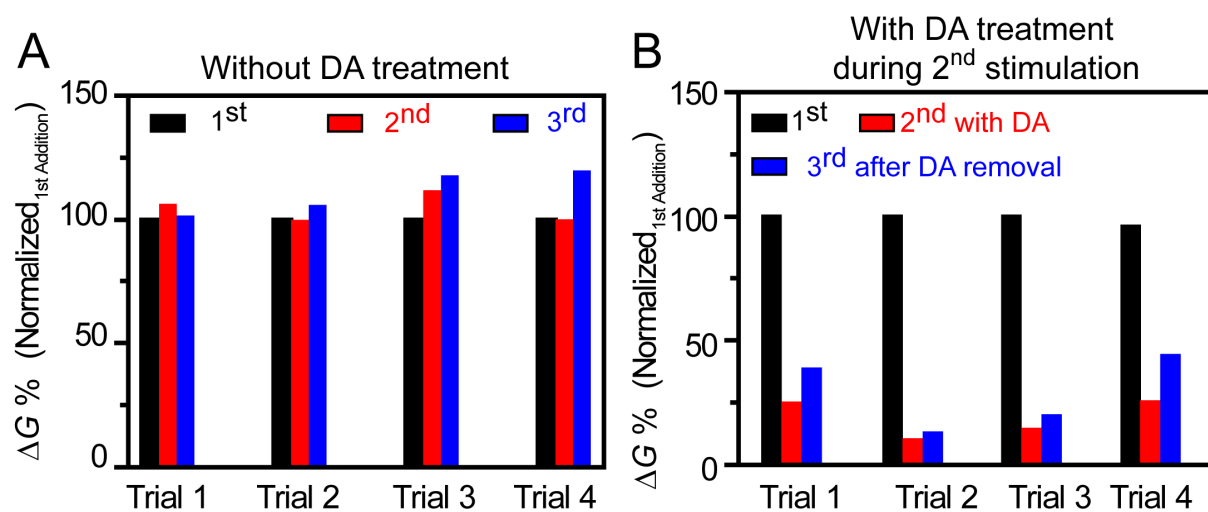


Figure S6. DA attenuated the histamine-induced NPY secretion. PC12 cells atop an APT^{NPY}/SiNW-FET were stimulated repeatedly by histamine (1.7 μM) 3 times in the conditions of A) DA absence ($C_{\text{DA}} = 0 \mu\text{M}$) and B) DA presence ($C_{\text{DA}} = 20 \mu\text{M}$) during the 2nd stimulation. Before the 3rd stimulation, the added DA was washed away. The normalized ΔG data were collected during the 3 stimulations from 4 different devices

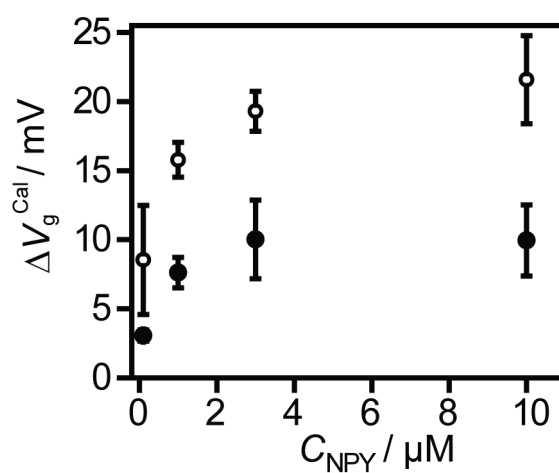


Figure S7. DA attenuates the sensitivity of an APT^{NPY}/SiNW-FET. The APT^{NPY}/SiNW-FET was perfused with various C_{NPY} in the presence ($C_{\text{DA}} = 20 \mu\text{M}$, filled circles) or absence ($C_{\text{DA}} = 0 \mu\text{M}$, empty circles) of DA. The calibrated response (ΔV_g^{cal}) is plotted against C_{NPY} . Data presented are the mean \pm standard deviation from at least 3 different devices.

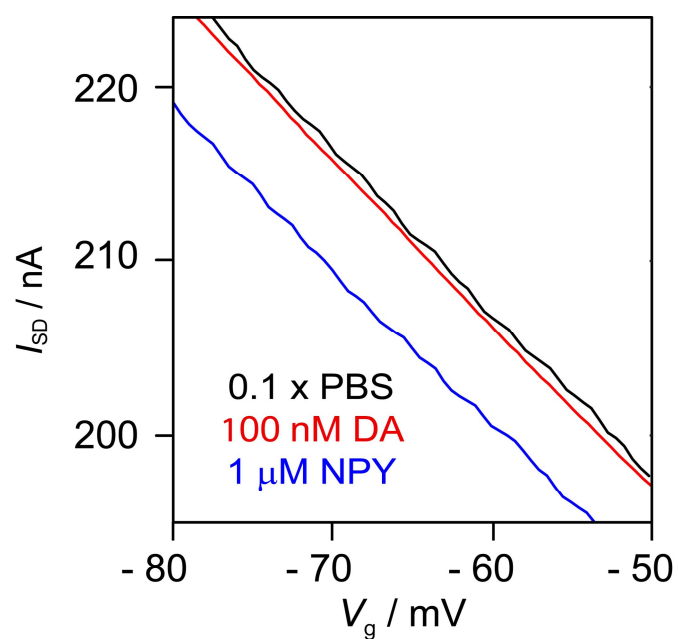


Figure S8. $I_{sd}-V_g$ curves of an APT^{NPY}/SiNW-FET in response to a 0.1× PBS buffer (black curve), a buffer containing 100 nM of DA (red curve), and a buffer containing 1 μM of NPY (blue curve).

Reference

- [S1] S. D. Mendonsa, M. T. Bowser, *J. Am. Chem. Soc.* **2005**, *127*, 9382.
- [S2] C. Mannironi, A. Di Nardo, P. Fruscoloni, G. P. Tocchini-Valentini, *Biochemistry* **1997**, *36*, 9726.
- [S3] G. Frens, *Nat. Phys. Sci.* **1973**, *241*, 20.
- [S4] K.-I. Chen, B.-R. Li, Y.-T. Chen, *Nano Today* **2011**, *6*, 131.
- [S5] T.-W. Lin, P.-J. Hsieh, C.-L. Lin, Y.-Y. Fang, J.-X. Yang, C.-C. Tsai, P.-L. Chiang, C. -Y. Pan, Y.-T. Chen, *Proc. Natl. Acad. Sci. U.S.A.* **2010**, *107*, 1047.
- [S6] R. S. Wagner, W. C. Ellis, *Appl. Phys. Lett.* **1964**, *4*, 89.
- [S7] Y.-H. Yang, S.-J. Wu, H.-S. Chiu, P.-I. Lin, Y.-T. Chen, *J. Phys. Chem. B* **2003**, *108*, 846.
- [S8] A. Javey, S. W. Nam, R. S. Friedman, H. Yan, C. M. Lieber, *Nano Lett.* **2007**, *7*, 773.
- [S9] K.-S. Chang, C.-J. Sun, P.-L. Chiang, A.-C. Chou, M.-C. Lin, C. Liang, H.-H. Hung, Y.-H. Yeh, C.-D. Chen, C.-Y. Pan, Y.-T. Chen, *Biosens. Bioelectron.* **2012**, *31*, 137.
- [S10] B.-R. Li, Y.-J. Hsieh, Y.-X. Chen, Y.-T. Chung, C.-Y. Pan, Y.-T. Chen, *J. Am. Chem. Soc.* **2013**, *135*, 16034.